Structural origin of the low superconducting anisotropy of $Bi_{1.7}Pb_{0.4}Sr_2Ca_{0.9}Cu_2O_8$ crystals

Roman Gladyshevskii
Department of Inorganic Chemistry, Ivan Franko National University of Lviv, UA-79005 Lviv, Ukraine

Nicolas Musolino and René Flükiger
Department of Condensed Matter Physics, University of Geneva, CH-1211 Geneva, Switzerland
(Received 3 August 2004; published 22 November 2004)

The structure of $Bi_{1.7}Pb_{0.4}Sr_2Ca_{0.9}Cu_2O_8$ (T_c=93 K) was refined from x-ray single crystal diffraction data in space group *A*2*aa*, a=5.3852(9) Å, b=5.4286(9) Å, c=30.997(6) Å. For this composition, the crystal structure is free from the structural modulation connected with the presence of additional oxygen atoms in the BiO layers. The *c*-axis lattice parameter is slightly larger in (Bi,Pb)-2212 crystals than in Pb-free Bi-2212 crystals, but the complete structural refinement revealed an inhomogeneous redistribution of the inter-planar distances. In particular, the distance between the two neighboring BiO layers has significantly decreased in the modulation-free phase as compared to the Pb-free phase. We believe that this is a key point in understanding the widely observed reduction of the anisotropy in Bi-2212 by Pb-doping. The irreversibility line as well as the onset of the second magnetization peak in modulation-free (Bi,Pb)-2212 crystals were studied. Because of the strongly reduced value of the anisotropy, the 2D-3D crossover field value, H_{cr}, is significantly higher in (Bi,Pb)-2212 crsystals than in Bi-2212 crystals. As a direct consequence of the structural modifications induced by the removal of the modulation, the nature of the inter-layer coupling changes from electromagnetic in modulated Bi-2212 to Josephson in modulation-free (Bi,Pb)-2212. Annealing the (Bi,Pb)-2212 crystals under oxygen reintroduced the structural modulation.

DOI: 10.1103/PhysRevB.70.184522 PACS number(s): 74.72.Hs, 74.62.Bf, 74.25.Ha

I. INTRODUCTION

Among the different chemical classes of high temperature superconductors, the Bi-based cuprates attract great interest, not only because of their physical properties, but also due to the peculiarities of their crystal structures.[1] One of the representatives of this class, the compound of ideal composition $Bi_2Sr_2CaCu_2O_8$ (Bi-2212), focused attention as high-quality single crystals became available with a high transition temperature $T_c \sim 93$ K. The structure of Bi-2212 is strongly layered, with thick insulating BiO blocks intercalated between superconducting CuO_2 planes. Crystal structure refinements revealed the presence of an incommensurate modulation connected with a corrugation of the atomic layers. The origin of this modulation has been the subject of many discussions.[2–8] Some authors emphasize the mismatch between translation units of the CuO_2 and BiO layers; others attribute the origin of the modulation to additional oxygen atoms inserted in the BiO layers.

From a physical point of view, it soon appeared that the intrinsic properties of this material impose some severe limitations to its applications. As a result of its layered structure, the anisotropy of the material is very pronounced.[9] This, combined with high operational temperatures and a short coherence length ξ, dramatically enhances the importance of fluctuations while reducing the effectiveness of pinning. Consequently, great efforts have been made to improve the pinning properties in Bi-2212, and cation substitution has been revealed to be a rewarding path. Chong *et al.*[10] first reported that the partial substitution of Bi by Pb in Bi-2212 crystals leads to a significant enhancement of the critical current densities and of the irreversibility field. Transport measurements further revealed that Pb doping significantly reduces the resistivity anisotropy parameter $\gamma^2=\rho_c/(\rho_a\rho_b)^{1/2}$ of the phase.[11–13] The *c*-axis resistivity ρ_c was found to systematically decrease with Pb doping, and its behavior just above T_c to change from semiconducting to metallic. Several suggestions were made to explain this enhancement of the interlayer coupling due to the presence of Pb, such as an increase of the carrier numbers or the creation of an additional covalent type of bonding between the two neighboring BiO layers. However, the origin of this phenomenon is still not elucidated. Pb doping also affects the structural modulation of the Bi-2212 phase. The wavelength of the modulation was shown to increase with increasing Pb concentration.[14,15] Recently, we obtained heavily Pb-doped (Bi,Pb)-2212 crystals free of modulation.[16] In this work, we present a detailed structural analysis of this modulation-free phase, and a comparison of the irreversibility and disorder-induced transition lines of modulated Bi-2212 and modulation-free (Bi,Pb)-2212.

II. PREPARATION AND EXPERIMENTAL TECHNIQUES

The crystals investigated were Pb free Bi-2212, and Pb doped (Bi,Pb)-2212 with an actual Pb content of 0.39 per formula unit, as determined by EDX analysis in combination with TEM. Single crystals were grown by a slow cooling technique from mixtures of nominal compositions $Bi_{2.2}Sr_2CaCu_2O_z$ and $Bi_{1.4}Pb_{0.8}Sr_2CaCu_2O_z$ in $BaZrO_3$ crucibles under a protected atmosphere, using a vertical three-zone furnace. The details of the growth process are described elsewhere.[17] The T_c onset of our as-grown heavily Pb-doped crystals was found by ac-susceptibility measurements to be 93 K with a transition width of about 10 K. Any attempt to

sharpen the transition, while keeping the high T_c value, was unsuccessful. Either T_c was significantly reduced, or the phase decomposed under low oxygen pressure annealing. The as-grown Pb-free Bi-2212 crystals were annealed in air at 500 °C for 100 h. Their resulting T_c onset was 85 K with a $\Delta T_c = 1$ K. The typical size of the crystals was $2 \times 2 \times 0.05$ mm^3.

A fragment ($0.43 \times 0.12 \times 0.016$ mm^3) was cut from a large, plate-like (Bi,Pb)-2212 crystal and mounted on a Stoe IPDS I diffractometer (Mo $K\alpha$ radiation, graphite monochromator). 2379 reflections were collected out to $\theta = 26°$ ($-6 \leqslant h \leqslant 6, -6 \leqslant k \leqslant 6, -36 \leqslant l \leqslant 27$) in the φ-scan mode, yielding 475 unique reflections ($R_{int} = 0.095$). An analytical absorption correction was made considering the size and shape of the crystal ($\mu = 57.134$ mm^{-1}). The structure was refined by the least-squares method based on $|F|$ values using the Xtal3.7 system.[18] The 51 parameters, including anisotropic displacement parameters for the metal-atom sites, refined to $R = 0.094$ and $wR = 0.052$ [$w = 1/\sigma^2(|F_{rel}|)$], considering all unique reflections.

The magnetic measurements were performed using a commercial Quantum Design SQUID, and an Oxford Instruments VSM. Field-cooled (FC) and zero-field-cooled (ZFC) magnetization was measured in an external magnetic field ($H \| \mathbf{c}$) up to 50 kOe, using a short scan length of 2 cm. The remanent field achieved in the ZFC experiments was less than 0.2 Oe. A proper measurement of the irreversibility line in platelet crystals is complicated by the existence of surface barriers and geometrical barriers, which may provide a significant contribution to the irreversible magnetization, even in the absence of bulk pinning. According to Zeldov *et al.*,[19] overcoming the geometrical barriers in a thin crystal of rectangular shape involves macroscopic energies, so that the thermal activation of the vortices over these barriers should be very weak. This has been observed experimentally in Bi-2212 crystals with this geometry, where no significant creep of the vortices was noted over four decades of time (logarithmic scale), and for various temperatures.[20] However, our previously reported measurements of the lower critical field H_{c1} of (Bi,Pb)-2212 crystals have shown that the field at which flux first penetrates the sample depends on the temperature and on the characteristic time of the experiment. This shows that thermal activation of vortices over the barriers is significant, and consequently rules out a geometrical nature of the barriers in these crystals. The influence of surface barriers would be revealed by an irreversibility field with values depending on the characteristic time of the experiment. To check this point, we have acquired FC-ZFC data at different temperature sweep rates. As a result, we see that the position of the irreversibility line (IL) is independent of the characteristic time of the experiment. This confirms the fact that there is no underlying relaxation process influencing the position of the IL, at least within the experimental time window.

III. CRYSTAL STRUCTURE

A. Structure of Bi-2212

We previously refined[6] the average structure of Pb-free Bi-2212 in the orthorhombic space group *A*2*aa*, $a = 5.4161(20)$ Å, $b = 5.4112(7)$ Å and $c = 30.873(7)$ Å. The Bi atoms are distributed over two sites (55% and 45% occupancy), the distance between the partly occupied sites being 0.59 Å. The deformation of the BiO layers with respect to an ideal rocksalt-type atom arrangement corresponds to a decrease of the number of O atoms that surround a Bi atom from six to three. The Bi atoms hence achieve a ψ-tetrahedral coordination, which is typical for Bi^{3+}. The lone electron pairs are situated between the BiO layers, which are thus only weakly connected.

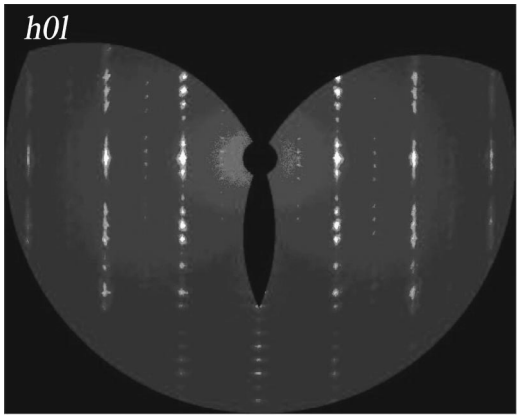

FIG. 1. X-ray diffraction patterns, taken with an imaging plate, of an as-grown single crystal of composition $Bi_{1.7}Pb_{0.4}Sr_2Ca_{0.9}Cu_2O_{8+\delta}$.

The real structure of Bi-2212 is modulated, as indicated by satellite diffraction reflections. The atom arrangement changes from one extreme configuration (square mesh) to another (chains) with a certain periodicity. In the *A*2*aa* description, the modulation vector $\mathbf{q} = 0.21\mathbf{a}^* + 0.14\mathbf{c}^*$ has a small but significant component along **c**, which corresponds to a translation period of ~220.5 Å. The structure is thus mainly characterized by an incommensurate modulation in the direction of one of the short translation vectors, with a translation period of about 4.76 translation units of the average lattice. Taking into consideration the satellite reflections, we refined the structure in the monoclinic space group *Cc* using a large monoclinic cell, 9 times larger than the unit cell of the average structure, with $a = 37.754(7)$ Å, $b = 5.4109(8)$ Å, $c = 41.070(9)$ Å and $\beta = 103.58(2)°$. Additional O atoms were detected in the BiO layers so that the large monoclinic unit cell contains $9 \times 30 + 4 = 274$ atoms (refined composition $Bi_{2.09(2)}Sr_{1.90(2)}Ca_{1.00(4)}Cu_2O_{8.22}$). This incorporation of extra O atoms may be considered as the main factor causing the structural modulation.

B. Structure of (Bi,Pb)-2212

Diffraction patterns of the Pb-doped (Bi,Pb)-2212 crystal are shown in Fig. 1. The absence of satellite reflections for the as-grown crystal indicates that the 0.39 Pb atoms per formula unit have removed the structural modulation present for Pb-free Bi-2212. The structure was refined in the noncentrosymmetric space group *A*2*aa*, cell parameters $a = 5.3852(9)$ Å, $b = 5.4286(9)$ Å, and $c = 30.997(6)$ Å. The final atom coordinates, displacement parameters, and occupa-

TABLE I. Atomic coordinates, equivalent or isotropic displacement parameters (Å^2), and occupation parameters in the structure $Bi_{1.7}Pb_{0.4}Sr_2Ca_{0.9}Cu_2O_8$ [space group *A*2*aa*, $a=5.3852(9)$ Å, $b=5.4286(9)$ Å, $c=30.997(6)$ Å].

Site	Wyckoff position	x	y	z	$U_{eq/iso}$[a]	Occ.
Bi1[b]	8d	0.011(2)	0.2653(4)	0.04990(6)	0.021(2)	0.91(2)
Bi2[b]	8d	0.124(14)	0.275(4)	0.0506(8)	0.021(2)[c]	0.09(2)[d]
Sr	8d	0.529(3)	0.2469(3)	0.1400(1)	0.030(3)	1
Cu	8d	0	0.2508(4)	0.1966(1)	0.018(2)	1
Ca[e]	4c	0.497(4)	0.25	0.25	0.016(5)	1
O1	8d	0.628(7)	0.343(5)	0.0535(12)	0.060(8)	1
O2	8d	−0.005(13)	0.225(3)	0.1151(8)	0.031(6)	1
O3	8d	0.25	0.496(15)	0.1991(6)	0.035(6)	1
O4	8d	0.25	0.000(15)	0.2007(6)	0.034(5)	1

[a] $U_{eq}=1/3\Sigma_i\Sigma_j a_i^* a_j^* \mathbf{a_i}\cdot\mathbf{a_j}$.
[b] $Bi1\equiv Bi2\equiv Bi_{0.8}Pb_{0.2}$.
[c] Constraint $U_{ij}(Bi2)=U_{ij}(Bi1)$.
[d] Constraint occ.(Bi2)+occ.(Bi1)=1.
[e] $Ca\equiv Ca_{0.90(1)}Bi_{0.10(1)}$.

tion factors are listed in Tables I and II. The starting model corresponded to the ideal structure of Bi-2212. The Bi/Pb ratio was fixed to 0.8/0.2, based on EDX analysis. Residual electron density was found in the Bi layer, which led us to introduce an additional Bi site (Bi2). Its occupancy was rather low and was constrained in the refinement to give a total of 100% for the two Bi sites. This site splitting is similar to that observed for modulated Pb-free Bi-2212 and indicates that the crystal under investigation is not completely free of modulation, but contains some stacking faults ($\simeq 9\%$). Stacking faults in the form of lamellas of the modulated phase were observed on TEM and STM images of crystals with a slightly lower Pb content.[16,21,22] The presence of stacking faults in our crystals may also explain the relatively broad superconducting transition and the presence of a significant amount of disorder (see Sec. IV).

The two Bi sites show the largest difference in the *x* coordinates, which is in agreement with a modulation direction along **a**, the distance between the two partly occupied sites being 0.61 Å. The relatively high equivalent displacement parameter of the Sr site, which is due to a high component along **a**, can be explained in a similar way. The same is also true for the displacement parameter of the oxygen site in the BiO layer (O1). The Cu site, as well as the oxygen sites in the CuO_2 layers (O3 and O4), showed no displacement in the **a** direction, with respect to the ideal structure, and their coordinates were fixed at the final stage of the refinement. Attempts to refine a partial substitution of Sr by Ca revealed no Ca on this site, whereas 10% substitution by Bi was found on the Ca site, located between the CuO_2 layers. This gives the final composition $Bi_{1.70(1)}Pb_{0.4}Sr_2Ca_{0.90(1)}Cu_2O_8$.

It has already been observed that substitution of Bi by Pb in Bi-2212 is accompanied by an increase of the modulation period.[14,15] For example, for a Pb content of 0.3 atoms per formula unit, the modulation vector was increased from 4.76 to approximately 10. The relative occupancies of the two Bi sites introduced here can be used to quantify the modulation. The values obtained for the crystal containing 0.39 Pb atoms per formula unit studied here (91% and 9%), can be compared with those obtained from the refinement on a single crystal with a Pb content of 0.34 atoms per formula unit (84% and 16%).[23] For a Pb content close to 0.44 atoms per formula unit, the periodicity of the structural modulation is expected to become infinite. Modulation-free structures have also been reported[24] for samples of composition $Bi_{2-x}Pb_xSr_2Y_{1-y}Ca_yCu_2O_z$ in the region $x=(1-y/2)\pm 0.2, 0\leqslant y\leqslant 0.8$. These structures, refined in space group *Pnan*, revealed a large orthorhombic distortion ($a/b=0.9913$ for $x=0.8$, $y=0.4$, and $z=8$) and directly superposed chains in consecutive BiO layers (in the structure of Y-free Bi-2212, the chains are mutually shifted by $\mathbf{a}/2$).

TABLE II. Anisotropic displacement parameters (Å^2) of the metal-atom sites in the structure of $Bi_{1.7}Pb_{0.4}Sr_2Ca_{0.9}Cu_2O_8$ (space group *A*2*aa*).

Site	U_{11}	U_{22}	U_{33}	U_{12}	U_{13}	U_{23}
Bi[a]	0.025(4)	0.0213(6)	0.0157(5)	−0.012(2)	−0.002(2)	−0.0004(4)
Sr	0.044(5)	0.026(2)	0.018(1)	0.003(2)	0.000(5)	−0.0017(8)
Cu	0.023(3)	0.020(2)	0.013(2)	−0.026(3)	−0.005(4)	0.0003(9)
Ca	0.010(6)	0.022(5)	0.015(3)	0	0	−0.001(2)

[a] $U_{ij}(Bi)=U_{ij}(Bi1)=U_{ij}(Bi2)$.

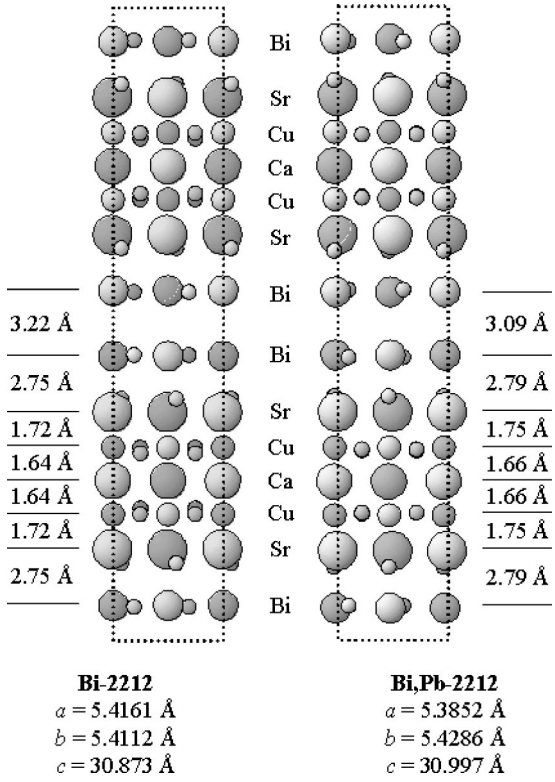

FIG. 2. Structures of Bi-2212 (average) and (Bi,Pb)-2212 in projections along [010]. The large circles are cations and the small circles are oxygen atoms.

C. Comparison of Bi-2212 and (Bi,Pb)-2212

It can be seen from Fig. 2 that the unit cell parameter along the stacking direction is slightly larger for (Bi,Pb)-2212 than for the Pb-free phase ($\Delta c = 0.124$ Å). Considering that there are 14 layers in the translation unit, the mean increase per layer is very small, less than 0.01 Å. However, a closer analysis of the crystal structure reveals an inhomogeneous distribution of the overall increase. The distance between the two Bi layers has in fact decreased by 0.13 Å, whereas all other inter-layer distances have increased by 0.02–0.04 Å. Even shorter distances between Bi layers have been reported[24] for modulation-free Y-containing (Bi,Pb)-2212. The decrease of the distance between the Bi layers is in agreement with the fact that these layers are no longer corrugated, but planar. The bonds between the Bi atoms and the O atoms belonging to the neighboring Sr layers (site O2), which represent the shortest Bi-O distances in the structure, have become approximately perpendicular to the Bi layer. This explains the increase of the corresponding inter-layer distance. The average angle between the Bi-O2 bonds and the plane formed by the Bi atoms is 82.6°, which can be compared with the corresponding angle 76.9° in Bi-2212. These structural changes are accompanied by an increase of the orthorhombicity [$a/b = 1.0009(5)$ and 0.9920(3) for Bi-2212 and (Bi,Pb)-2212, respectively].

Figure 3 shows a projection of two consecutive BiO layers along the [010] (nonmodulated) direction, and a projection of the lower layer (two identical chains) along the stacking direction, for modulated Pb-free Bi-2212. The periodicity along the [101] diagonal of the large monoclinic cell, indicated by the long arrow, corresponds to two translation units of the modulation wave (the dotted lines delimit the orthorhombic unit cell of the average structure). The figure shows the periodic change from zigzag chains of corner-linked ψ-tetrahedra to a rocksalt-type atom arrangement. The displacement of the Bi sites from the ideal rock-salt positions, perpendicular to the atom layers (transverse) and parallel to the modulation direction (longitudinal), are represented by graphs. They are described by sinusoidal curves where the maxima of the transverse displacement wave correspond to zero amplitude of the longitudinal displacement wave, and *vice versa*. The displacement of the oxygen atoms along the chains is described by a saw-like function, a linear section of which is shown by a dashed line. At a certain point, the displacement has become so large that an additional oxygen atom can be inserted. The result appears as a splitting of the ideal O site for a rocksalt-type arrangement into two sites (see the small arrows). The insertion of an additional O atom takes place every ninth Bi atom and defines the translation unit of the modulation wave. Thus, the actual composition of the layer is Bi_9O_{10} ($Bi_2O_{2.22}$ per formula unit), leading to a

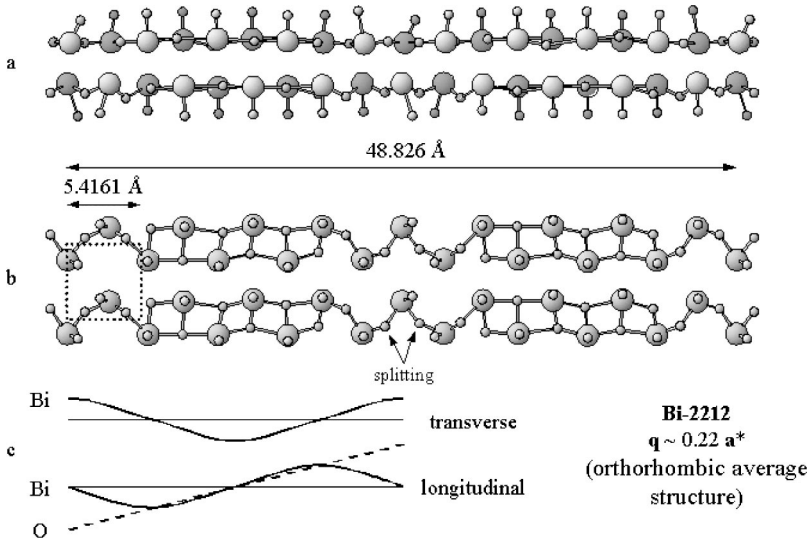

FIG. 3. Projection of (a) two consecutive BiO layers along [010] and (b) one BiO layer (two identical chains) along the stacking direction for modulated Bi-2212. The graph (c) shows the displacement of the Bi and O atoms from the ideal rocksalt positions.

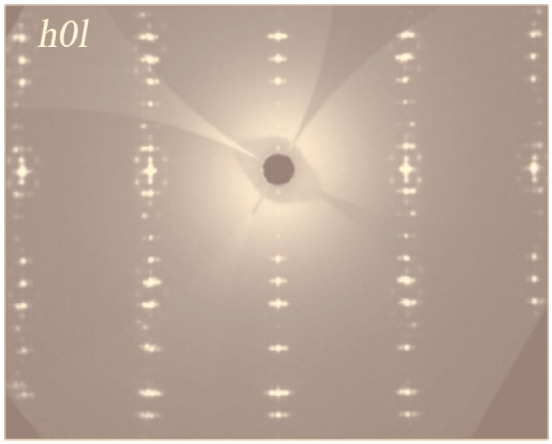

FIG. 4. X-ray diffraction patterns, taken with an imaging plate, of a single crystal of composition $Bi_{1.7}Pb_{0.4}Sr_2Ca_{0.9}Cu_2O_{8+\delta}$ annealed in oxygen.

total oxygen content 8.22 per formula unit. This deviation from electro-neutrality, which is partially compensated for by the presence of Bi^{3+} in the Ca layers, is a crucial parameter for the existence of the superconducting phase. The partial elimination of oxygen by annealing under reducing conditions does not remove the modulation, but produces more serious structural changes, which are accompanied by a decrease of T_c for underdoped compositions. The same is true for heavily overdoped samples, where the modulation vector can be even larger and more interstitial O atoms can be incorporated into the BiO layers. By replacing part of the cations by chemically similar cations in a lower oxidation state, it is possible to keep the same electron concentration while removing the additional O atoms, and thus to suppress the modulation. This can be achieved by substituting 22% of Bi^{3+} by Pb^{2+}: $Bi_2^{3+}Sr_2CaCu_2O_{8.22} \rightarrow Bi_{1.56}^{3+}Pb_{0.44}^{2+}Sr_2CaCu_2O_8$. Figure 5 shows two projections of the BiO layers in modulation-free Pb-doped (Bi,Pb)-2212, which can be directly compared with the ones presented in Fig. 3 (the Bi2 site with 9% occupation has been ignored). The arrangement of Bi and O atoms can be considered as distorted rocksalt-type.

The EDX analysis of the Pb content indicated 19.5% substitution of Bi by Pb, which is in good agreement with the quasi-absence of modulation. Consequently, the oxygen content should be close to 8 atoms per formula unit. It seems reasonable to believe that modulation-free (Bi,Pb)-2212 cannot be underdoped by oxygen without causing serious structural changes. However, it may be overdoped, but the insertion of additional O atoms into the BiO layers would again produce a modulated structure. In order to test this hypothesis, we annealed the Pb-doped crystal in oxygen atmosphere at $T=500\,^{\circ}C$ for 100 h. The satellite reflections observed in Fig. 4 confirm that the structure of the annealed crystal is effectively modulated ($\mathbf{q} \simeq 0.10\mathbf{a}^*$). During the annealing, additional O has been introduced and the oxidation state of Pb has probably in part changed from 2+ to 4+. The formation of modulation-free (Bi,Pb)-2212 is thus expected to be favored at low partial oxygen pressures.

The interatomic distances for the metal atoms given in Table III are in agreement with expected values. The Bi atoms have three O atoms at shorter distances, confirming the distorsion of the octahedral coordination corresponding to the ideal rocksalt-type atom arrangement into a ψ-tetrahedron (Fig. 6).

TABLE III. Selected interatomic distances (Å) in the structure of $Bi_{1.7}Pb_{0.4}Sr_2Ca_{0.9}Cu_2O_8$.

Atoms	*d*	Atoms	*d*
Bi[a]—O2	2.04(2)	Bi[b]—O2	2.08(3)
—O1	2.11(4)	—O1	2.14(5)
—O1	2.22(3)	—O1	2.70(8)
—O1	3.29(4)	—O1	2.74(8)
—O1	3.35(4)	—O1	3.25(5)
—O1	3.36(3)	—O1	3.35(3)
Sr—O3	2.59(5)	Cu—O3	1.90(6)
—O4	2.60(4)	—O4	1.92(6)
—O2	2.62(7)	—O4	1.92(6)
—O2	2.68(2)	—O3	1.93(6)
—O3	2.73(4)	—O2	2.53(2)
—O4	2.76(4)	Ca[b]—2 O4	2.44(5)
—O1	2.78(4)	—2 O4	2.45(5)
—O2	2.98(2)	—2 O3	2.46(5)
—O2	2.98(7)	—2 O3	2.50(5)

[a]$Bi1 \equiv Bi2 \equiv Bi_{0.8}Pb_{0.2}$.
[b]$Ca \equiv Ca_{0.90(1)}Bi_{0.10(1)}$.

IV. MAGNETIC PROPERTIES

Figures 7 and 8 show the IL obtained for a modulated Bi-2212 crystal and for a modulation-free (Bi,Pb)-2212 crystal. The onset, H_{on}, of the second magnetization peak (SP), as determined from SQUID and VSM hysteresis loops, is marked by open squares. Looking at the shape of the IL line, one can observe a clear change in its temperature dependence at a characteristic magnetic field, which we label H_{cr}. This effect has been attributed to a change in the dimensionality of the vortex lattice from a 3D lattice at low fields to a

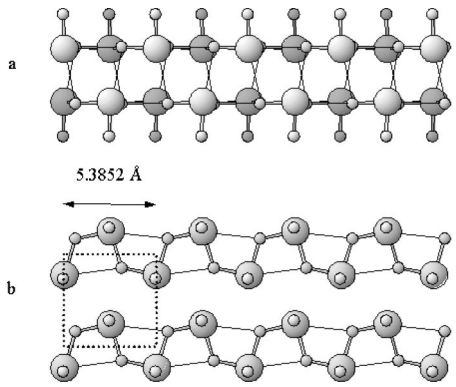

FIG. 5. Projections of (a) two consecutive BiO layers along [010] and (b) one BiO layer (two identical chains) along [001] for modulation-free (Bi,Pb)-2212.

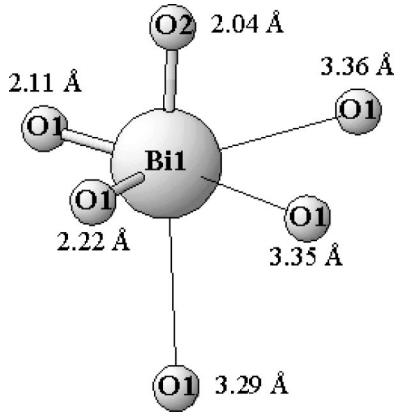

FIG. 6. Environment of the site Bi1 in modulation-free (Bi,Pb)-2212.

quasi-2D lattice at higher fields.[25] Below H_{cr}, the inter-plane interactions between pancake vortices are dominant, thus forming well defined 3D objects. Above H_{cr}, the in-plane interactions become dominant and the vortex lattice becomes essentially two dimensional.

The description of the crossover field H_{cr} depends on the origin of the main inter-plane interaction between the pancake vortices.[26] In strongly layered Bi-2212, the inter-plane coupling occurs via electromagnetic and Josephson interactions.[27,28] The characteristic length of the electromagnetic interaction is the electromagnetic in-plane penetration depth λ_{ab}. In the case of Josephson coupling, this characteristic length is given by γd, where γ is the anisotropy value and d is the distance between CuO_2 planes of consecutive slabs. If $\lambda_{ab} > \gamma d$, the Josephson interactions dominate and the crossover field is given by $H_{cr} \simeq \phi_0 / \gamma^2 d^2$. In the case

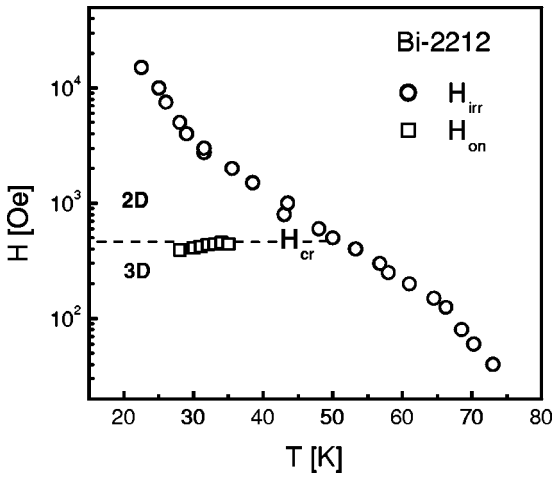

FIG. 7. Irreversibility line (H_{irr}) and the disorder-induced transition line of a Pb-free Bi-2212 crystal. The quasi-ordered Bragg glass phase forms at low magnetic fields, and is bounded by the onset of the second magnetization peak H_{on}. Above this transition, the system becomes entangled. Due to the very high anisotropy of the crystal, the entanglement also corresponds to a change in dimensionality of the vortex lattice, which becomes quasi-2D. This crossover is revealed by a clear change in the temperature dependance of the IL at a characteristic field, H_{cr} on the graph.

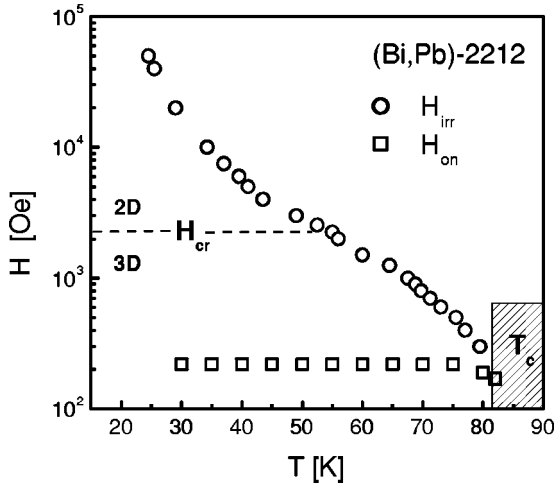

FIG. 8. Irreversibility line (H_{irr}) and disorder-induced transition line of a modulation-free Pb-doped (Bi,Pb)-2212 crystal. Note that the second magnetization peak extends up to T_c, with an onset field, H_{on}, which is nearly independent of the temperature up to $T = 75$ K. This is the signature of a large amount of disorder in the crystal. The entanglement transition no longer corresponds to the 2D-3D crossover, which occurs at a higher applied magnetic field.

$\lambda_{ab} < \gamma d$, the electromagnetic interactions take over and the crossover field is $H_{cr} \simeq \phi_0 / \lambda_{ab}^2$. For the Pb-free Bi-2212 crystals studied here, we measured[17] an anisotropy value of $\gamma = 165$, so that $\gamma d = 2500$ Å is of the order of the low-temperature value of the penetration depth.[29] This suggests that both interactions have to be taken into account. The experimentally found crossover field value $H_{cr} \simeq 450$ Oe is in good agreement with each of the two expressions introduced above. Aegerter *et al.*[30] have studied the dimensional crossover in Bi-2212 as a function of the oxygen content. Their results indicated that H_{cr} depends on the in-plane penetration depth λ_{ab}, rather than on the anisotropy γ, and thus point out that the electromagnetic inter-plane interactions between the pancake vortices are dominant. More recently, Correa, Kaul, and Nieva[26] published a study aiming to solve the controversy on the nature of the inter-layer coupling in Bi-2212. They showed that, close to optimal doping, inter-layer coupling is mainly electromagnetic and turns to Josephson character only for strong over-doping.

For the modulation-free (Bi,Pb)-2212 crystals, we see from the IL that the 2D-3D crossover occurs at a significantly higher applied magnetic field, $H_{cr} \simeq 2250$ Oe. The crossover expressions based on electromagnetic interactions yield an abnormally low value of the in-plane penetration depth, $\lambda_{ab} \simeq 960$ Å. Previous measurements[16] on modulation-free (Bi,Pb)-2212 led to a value $\lambda_{ab} \simeq 2000$ Å at $T = 30$ K. Using the crossover expression based on the Josephson interactions, we obtain an anisotropy value $\gamma = 63$, which self-consistently fills the condition $\gamma d < \lambda_{ab}$. We note, however, that this anisotropy value is larger than the one previously found experimentally,[16] $\gamma_{exp} \simeq 25$. Interestingly, this change in the nature of the inter-layer coupling is not a consequence of overdoping, but stems directly from the structural changes induced by the removal of the modulation. Indeed, the T_c onset of the modulation-free crystals corre-

sponds to the optimal doping state of Bi-2212, as the charge introduced in the system by the substitution $Bi^{3+} \rightarrow Pb^{2+}$ is compensated by the removal of the extra oxygen atoms. We thus conclude that the structural changes induced by the removal of the modulation, namely the shortening of the distance between the Bi atom planes, lead to a modification in the nature of the main inter-plane interaction between the pancake vortices from electromagnetic to Josephson type.

A second interesting difference between Pb-free and Pb-doped Bi-2212 crystals comes from the relationship between the SP line, H_{on}, and the position of the dimensional crossover, H_{cr}. The second-peak structure is the signature of a disorder-driven transition from the low-field/low-temperature long-range ordered Bragg glass to an entangled phase where dislocations proliferate.[31–34] This transition usually manifests itself by a sudden increase in the irreversible magnetization and is readily observed in magnetization hysteresis loops as a distinct second-magnetization peak.[35–37] Because of the extreme anisotropy of the Bi-2212 crystals, the entanglement of the vortex lattice also corresponds to a decoupling of the planes, as can be seen in Fig. 6 from the equivalence $H_{sp} = H_{cr} \simeq 450$ Oe. In (Bi,Pb)-2212, these two characteristic fields are clearly distinct, the lattice entering first the entangled regime at $H_{sp} = 220$ Oe before decoupling at a higher magnetic field $H_{cr} \simeq 2250$ Oe. In the Pb-doped (Bi,Pb)-2212 crystals, a significant amount of disorder is revealed by the persistence of the second-peak structure nearly up to T_c. An obvious consequence of an excess of disorder is to lower the field at which the disorder-induced transition occurs. Hence, in the (Bi,Pb)-2212 crystals, it is difficult to assess the role of the disorder and of the reduced anisotropy in the separation between the disorder-induced transition line and the decoupling line.

V. CONCLUSION

A partial substitution of Bi by Pb in Bi-2212 is accompanied by the removal of the additional O atoms in the BiO layers. For a replacement of ~20% of Bi^{3+} by Pb^{2+} the apparent translation unit of the structural modulation becomes infinite (no modulation). The BiO layers are no longer corrugated and the distance between neighboring Bi layers has decreased from 3.22 Å in Pb-free Bi-2212 to 3.09 Å in modulation-free heavily Pb-doped (Bi,Pb)-2212. As a direct consequence, the anisotropy of the modulation-free crystals is strongly reduced and the nature of the inter-layer coupling changes from electromagnetic in Pb-free Bi-2212 to Josephson-like in heavily Pb-doped (Bi,Pb)-2212. Annealing the crystals under oxygen reintroduces the structural modulation. The present study is thus in favor of attributing the origin of the structural modulation in Bi-based superconducting cuprates to the presence of additional oxygen atoms in the BiO layers.

ACKNOWLEDGMENTS

We would like to thank Dr. E. Walker for having grown the crystals and Dr. R. Černý for help with the x-ray data collection. This research was supported by the Swiss National Research Fund and the Swiss NCCR on Materials with Novel Electronic Properties (MaNEP).

[1] R. Gladyshevskii and P. Galez, in *Handbook Superconductivity*, edited by C. P. Poole, Jr. (Academic Press, San Diego, 2000).
[2] H. W. Zandbergen, W. A. Groen, F. C. Mijlhof, G. Van Tendeloo, and S. Amelinckx, Physica C **156**, 325 (1988).
[3] Y. Le Page, W. R. McKinnon, J. M. Tarascon, and P. Barboux, Phys. Rev. B **40**, 6810 (1999).
[4] V. Petricek, Y. Gao, P. Lee, and P. Coppens, Phys. Rev. B **42**, 387 (1990).
[5] Y. Gao, P. Coppens, D. E. Cox, and A. R. Moodenbaugh, Acta Crystallogr., Sect. A: Found. Crystallogr. **49**, 141 (1993).
[6] R. Gladyshevskii and R. Flükiger, Acta Crystallogr., Sect. B: Struct. Sci. **52**, 38 (1996).
[7] D. Grebille, H. Leligny, A. Ruyter, P. Labbé, and B. Raveau, Acta Crystallogr., Sect. B: Struct. Sci. **52**, 628 (1996).
[8] J. M. Perez-Mato, J. Etrillard, J. M. Kiat, B. Liang, and C. T. Lin, Phys. Rev. B **67**, 024504 (2003).
[9] J. C. Martinez, S. H. Brongersma, A. Koshelev, B. Ivlev, P. H. Kes, R. P. Griessen, D. G. de Groot, Z. Tarnavski, and A. A. Menovsky, Phys. Rev. Lett. **69**, 2276 (1992).
[10] I. Chong, Z. Hiroi, M. Izumi, J. Shimoyama, Y. Nakayama, K. Kishio, T. Terashima, Y. Bando, and M. Takano, Science **276**, 770 (1997).
[11] F. X. Régi, J. Schneck, H. Savary, R. Mellet, and C. Daguet, Appl. Supercond. **1**, 627 (1993).
[12] L. Winkeler, S. Sadewasser, B. Beschoten, H. Frank, F. Nouvertné, and G. Güntherodt, Physica C **265**, 194 (1996).
[13] T. Motohashi, Y. Nakayama, T. Fujita, K. Kitazawa, J. Shimoyama, and K. Kishio, Phys. Rev. B **59**, 14080 (1999).
[14] N. Fukishima, H. Niu, S. Nakamura, S. Takeno, M. Hayashi, and K. Ando, Physica C **159**, 777 (1989).
[15] O. Eibl, Physica C **175**, 419 (1991).
[16] N. Musolino, S. Bals, G. van Tendeloo, N. Clayton, E. Walker, and R. Flükiger, Physica C **399**, 1 (2003).
[17] N. Musolino, S. Bals, G. van Tendeloo, N. Clayton, E. Walker, and R. Flükiger, Physica C **401**, 270 (2004).
[18] *Xtal3.7 system*, edited by S. R. Hall, D. J. du Boulay, and R. Olthof-Hazekamp, University of Western Australia, 2000.
[19] E. Zeldov, A. I. Larkin, V. B. Geshkenbein, M. Konczykowski, D. Majer, B. Khaykovich, V. M. Vinokur, and H. Shtrikman, Phys. Rev. Lett. **73**, 1428 (1994).
[20] M. Nideröst, R. Frassanito, M. Saalfrank, A. C. Mota, G. Blatter, V. N. Zavaritsky, T. W. Li, and P. H. Kes, Phys. Rev. Lett. **81**, 3231 (1998).
[21] Z. Hiroi, I. Chong, and M. Takano, J. Solid State Chem. **138**, 98 (1998).
[22] G. Kinoda, T. Hasegawa, S. Nakao, T. Hanaguri, K. Kitazawa, K. Shimizu, J. Shimoyama, and K. Kishio, Phys. Rev. B **67**, 224509 (2003).
[23] R. Gladyshevskii, O. Shcherban, and R. Flükiger, Visn. Lviv Univ. Ser. Khim. **39**, 201 (2000).

[24] G. Calestani, M. G. Franchesconi, G. Salsi, and G. D. Andreetti, Physica C **197**, 283 (1992).
[25] A. Schilling, R. Jin, J. D. Guo, and H. R. Ott, Phys. Rev. Lett. **71**, 1899 (1993).
[26] V. F. Correa, E. E. Kaul, and G. Nieva, Phys. Rev. B **63**, 172505 (2001).
[27] W. E. Lawrence and S. Doniach, *Proceedings of the XII International Conference on Low Temperature Physics*, 1970, p. 361.
[28] J. R. Clem, Phys. Rev. B **43**, 7837 (1991).
[29] V. G. Kogan, M. Ledvij, A. Y. Simonov, J. H. Cho, and D. C. Johnston, Phys. Rev. Lett. **70**, 1870 (1993).
[30] C. M. Aegerter, S. L. Lee, H. Keller, E. M. Forgan, and S. H. Lloyd, Phys. Rev. B **54**, R15661 (1996).
[31] T. Giamarchi and P. Le Doussal, Phys. Rev. B **55**, 6577 (1997).
[32] T. Giamarchi and S. Bhattacharya, in *High Magnetic Fields—Application in Condensed Matter Physics and Spectroscopy* (Springer-Verlag, Berlin, 2001), pp. 314–360.
[33] V. Vinokur, B. Khaykovich, E. Zeldov, M. Konczykowski, R. A. Doyle, and P. H. Kes, Physica C **295**, 209 (1998).
[34] J. Kierfeld and V. Vinokur, Phys. Rev. B **61**, R14928 (2000).
[35] M. Baziljevich, D. Giller, M. McElfresh, Y. Abulafia, Y. Radzyner, J. Schneck, T. H. Johansen, and Y. Yeshurun, Phys. Rev. B **62**, 4058 (2000).
[36] Y. Yamaguchi, N. Shirakawa, G. Rajaram, K. Oka, A. Mumtaz, H. Obara, T. Nakagawa, and H. Bando, Physica C **361**, 244 (2001).
[37] V. F. Correa, G. Nieva, and F. de la Cruz, Phys. Rev. Lett. **87**, 057003 (2001).